MULTI-EXCITATION HYPERSPECTRAL IMAGING FOR NON-DESTRUCTIVE QUALITY CONTROL OF COLLAGEN SCAFFOLDS

Ani Avetisyan[1], Kristina Ghahramanyan[1], Tigran Soghomonyan[1], Fernando Villarruel[1], Ekaterina Baidiuk[1], Narine Sarvazyan[1,2]

[1]L.A. Orbeli Institute of Physiology NAS RA, Yerevan, Armenia
[2]The George Washington University School of Medicine and Health Sciences, Washington, DC, USA

ABSTRACT

Collagen scaffolds are widely used in tissue engineering, and the degree of chemical crosslinking determines their stability, degradation rate and biocompatibility. Tools that verify crosslinking non-destructively and across the whole scaffold are lacking. We tested whether multi-excitation hyperspectral imaging (ME-HSI), which adds excitation wavelength as a fourth dimension to conventional hyperspectral dataset, can detect crosslinking-dependent changes in collagen autofluorescence. Sponges made from bovine tendon type I collagen, extracted with or without pepsin, were crosslinked with glutaraldehyde at three concentrations and imaged at six excitation wavelengths (310–400 nm) and 31 emission bands (420–720 nm). Mean spectra of the three groups were very similar, yet pixel-level support vector machine classification separated the crosslinking levels with accuracies of up to 95%, and combining excitations outperformed single excitations. The most discriminative excitations depended on the collagen extraction method. ME-HSI is a promising non-destructive tool for spatially resolved quality control of collagen biomaterials.

***Index Terms*—** multi-excitation hyperspectral imaging, autofluorescence, collagen scaffold, glutaraldehyde crosslinking, support vector machine.

1. INTRODUCTION

Type I collagen is the main structural protein of the extracellular matrix and the most widely used natural material for tissue-engineering scaffolds, owing to its biocompatibility and biodegradability [1]. Scaffolds made from purified collagen are usually crosslinked to increase their mechanical strength and slow their enzymatic degradation, and glutaraldehyde remains one of the most common crosslinking agents [2]. The degree of crosslinking has to be controlled: insufficient crosslinking yields a scaffold that degrades too quickly, whereas excessive glutaraldehyde treatment stiffens the matrix and raises cytotoxicity concerns [2]. The extraction protocol matters as well; acid-solubilized and pepsin-aided extraction of bovine tendon collagen produce fibrils with different structural characteristics [3]. Standard methods for assessing crosslinking, such as thermal denaturation or free-amine assays, are destructive and report a bulk average, while the spatial homogeneity of a scaffold is often what determines its performance.

Collagen is intrinsically fluorescent under ultraviolet (UV) excitation, and its autofluorescence reflects the state of the protein, including its crosslinks and enzymatic degradation [4], [5]. Chemical crosslinking with glutaraldehyde also generates new fluorescent products. Changes in autofluorescence could therefore serve as a label-free readout of scaffold crosslinking, provided that the relevant spectral differences can be detected and mapped.

Hyperspectral imaging (HSI) records a spectrum at every pixel and is increasingly used in biomedical applications, including wound assessment [6], [7]. Fluorescence HSI is typically performed with a single excitation wavelength, which limits its ability to separate fluorophores with overlapping emission. Multi-excitation HSI (ME-HSI) acquires a stack of emission cubes under several excitation wavelengths, producing a four-dimensional dataset (x, y, λ_{ex}, λ_{em}). Our group has shown that ME-HSI improves discrimination of nerve from ligament [8], [9] and of lichen species [10] relative to single-excitation imaging. Here we asked two questions: 1) whether ME-HSI can detect the impact of glutaraldehyde crosslinking in collagen sponges prepared by two extraction methods, and 2) which excitation wavelengths carry the most discriminative information.

2. MATERIALS AND METHODS

2.1. Collagen sponge preparation

Type I collagen was extracted from bovine tendon (Fig. 1) following the modified acid-solubilized and pepsin-aided procedures of Ju et al. [3], with all steps carried out at 4 °C. Tendons were cleaned of muscle, fascia, and fat, cut into 2 mm slices, and soaked for 48–72 h in PBS. For Prep A (without pepsin), the slices were acidified in 0.5 M acetic acid at a solid/solvent ratio of 1:20 (w/v) for 48–72 h with stirring and then centrifuged (10,000 × g, 30 min); the residue was re-extracted in 0.5 M acetic acid (1:20, w/v) for 48 h. For Prep B (with pepsin), acidification was performed in 0.5 M acetic acid at 1:20 (w/v) with pepsin added under

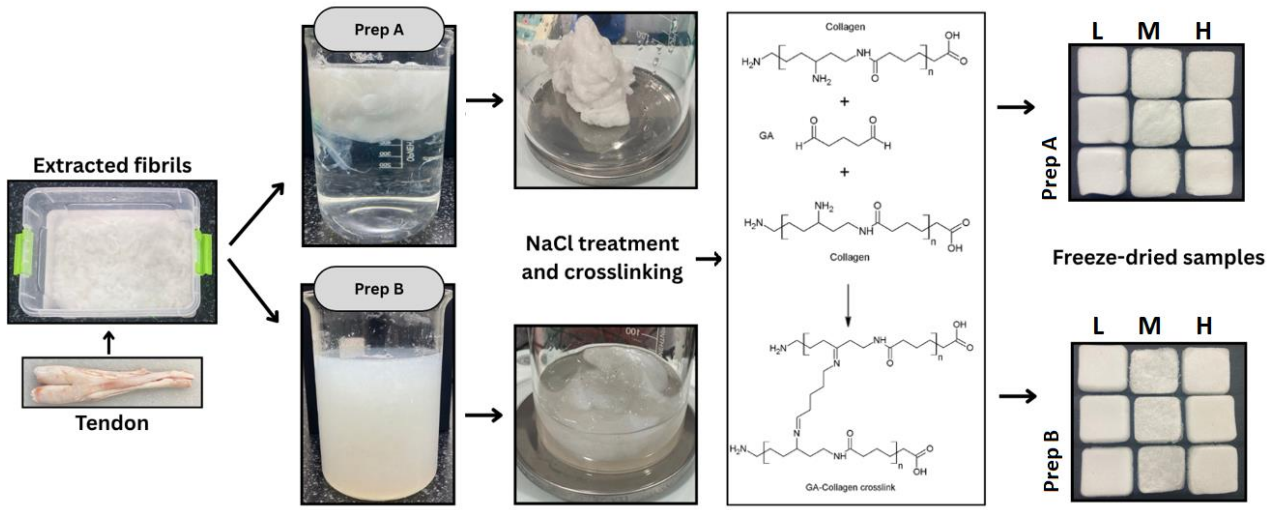


Fig. 1. Preparation of collagen sponges. Collagen fibrils extracted from bovine tendon were solubilized without (Prep A) or with pepsin (Prep B), treated with NaCl and crosslinked with glutaraldehyde (GA), which links lysine amino groups of adjacent collagen chains through Schiff-base (imine) bonds, and then freeze-dried. Right: 2x2cm freeze-dried sponges with three samples arranged vertically for each GA concentration (0.002%, 0.0075%, or 0.13%) marked as low, medium, and high, respectively.

magnetic stirring for 48–72 h. The suspension was centrifuged (10,000 × g, 30 min), the supernatant was collected, and solubilized collagen was precipitated by gradual addition of NaCl to a final concentration of 0.7 M. After 24 h of gentle agitation at 4 °C, the precipitate was collected and redissolved in 0.5 M acetic acid. The solution was dialyzed against cold deionized water (200:1, v/v) for three days using SpectraPor® membranes (MWCO 12–14 kDa), with daily water changes. Collagen solutions containing 0.5% collagen and glutaraldehyde at 0.002%, 0.0075%, or 0.13% (low, medium, and high, respectively) were cast into molds, stored at −80 °C for 24 h, and freeze-dried (**Fig. 1**). Three sponges per crosslinking concentration were arranged in a 3 × 3 array and imaged together.

2.2. ME-HSI acquisition

Images were acquired with a Nuance FX hyperspectral camera (CRi/PerkinElmer) fitted with a liquid-crystal tunable filter (**Fig.2**). Samples were illuminated sequentially by narrow-band UV LEDs (Mightex) centered at 310, 325, 340, 365, 385 and 400 nm. For each excitation, an emission cube was recorded from 420 to 720 nm in 10 nm steps (31 bands). The six cubes together form one ME-HSI dataset per preparation.

2.3. Data analysis

Pixel spectra were extracted from regions of interest covering each sponge and normalized to their maximum per cube. To visualize class separability, t-distributed stochastic neighbor embedding (t-SNE) [11] was applied to the pixel spectra of each excitation separately.

Pixel-level classification into the three crosslinker levels was performed with a support vector machine (SVM) using a radial basis function kernel [12]. The training set consisted of 3% random pixels taken from the top single samples per class, while all other pixels were used for testing and validation. Classification variables consisted of the 31 emission band values for each pixel. Performance is reported as classification accuracy, mean ± SD.

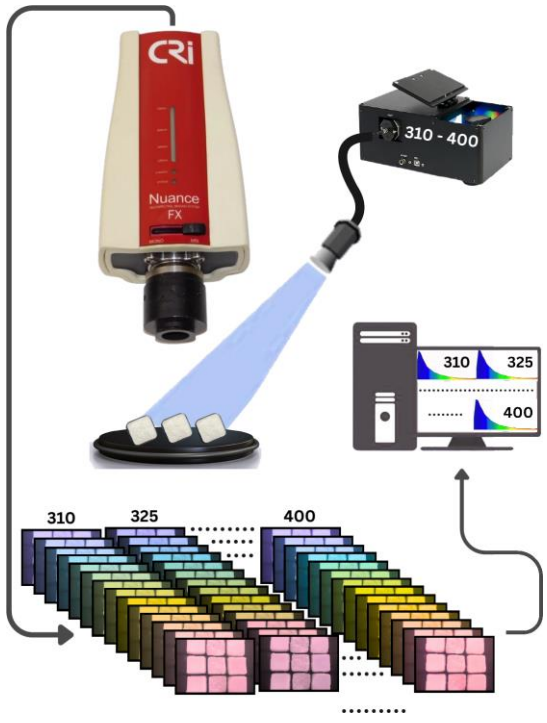


Fig. 2. ME-HSI setup. A Nuance FX camera records emission cubes (420–720 nm) under sequential excitation at 310–400 nm; the stack of cubes is analyzed pixel by pixel.

3. RESULTS

3.1. Spectral differences between crosslinking levels

In the t-SNE embeddings, pixels from the three crosslinker levels formed distinct clusters under 310, 325 and 340 nm excitation (**Fig. 3**). At 365 and 385 nm the high-crosslinker pixels were clearly separated from the low and medium groups, which partly overlapped. At 400 nm the three classes largely overlapped for both groups. These patterns indicate that the spectral data contain sufficient information to distinguish the classes at most excitation wavelengths.

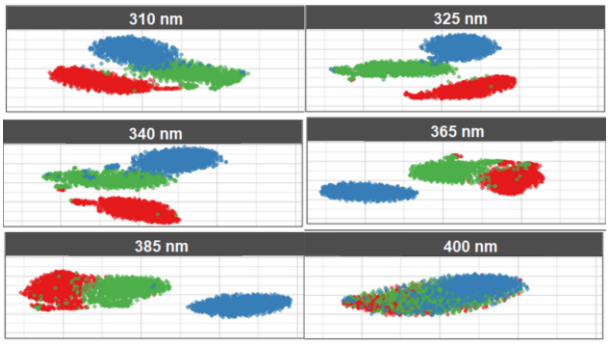


Fig. 3. t-SNE embeddings of pixel spectra acquired at each excitation wavelength for samples from Prep A series. Red, green and blue colors correspond to low, medium and high glutaraldehyde concentrations respectively.

The mean normalized emission spectra of the three groups were very similar at 310–340 nm excitation, all peaking near 430–440 nm (**Fig. 4**). Larger differences appeared at 365 and 385 nm, where the emission between approximately 450 and 550 nm rose with crosslinker concentration relative to the peak, so that the classes became visually identifiable. At 400 nm the low-crosslinker spectrum differed from the medium and high spectra, which nearly coincided.

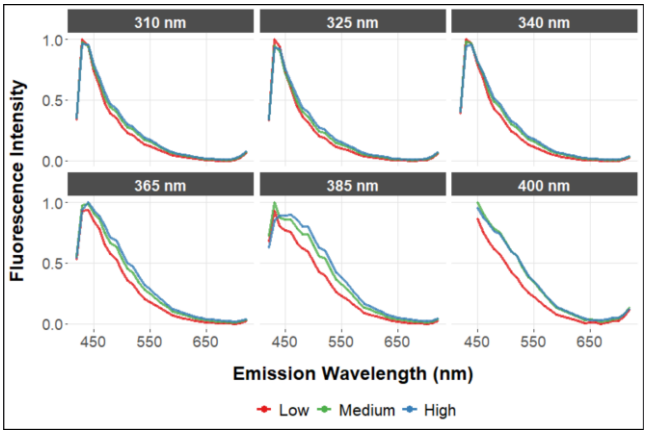


Fig. 4. Normalized mean emission spectra of collagen scaffolds made using Prep A (without pepsin) protocol crosslinked at low, medium and high glutaraldehyde concentration, for each excitation wavelength.

3.2. Classification with single excitations

For collagen samples prepared without pepsin (Prep A), SVM classification using the three best single excitations (325, 365, and 385 nm) achieved accuracies of 78%, 85%, and 85%, respectively (**Fig. 5a**). In comparison, pepsin-treated collagen (Prep B) exhibited better separability, with mean accuracies of 90%, 93%, and 94% at its three best excitations (310, 325, and 340 nm). Misclassified pixels appeared predominantly as scattered points inside individual sponges and along their edges. Per-class accuracies for best excitation are summarized in **Fig. 5b** (385 nm for Prep A, 340 nm for Prep B).

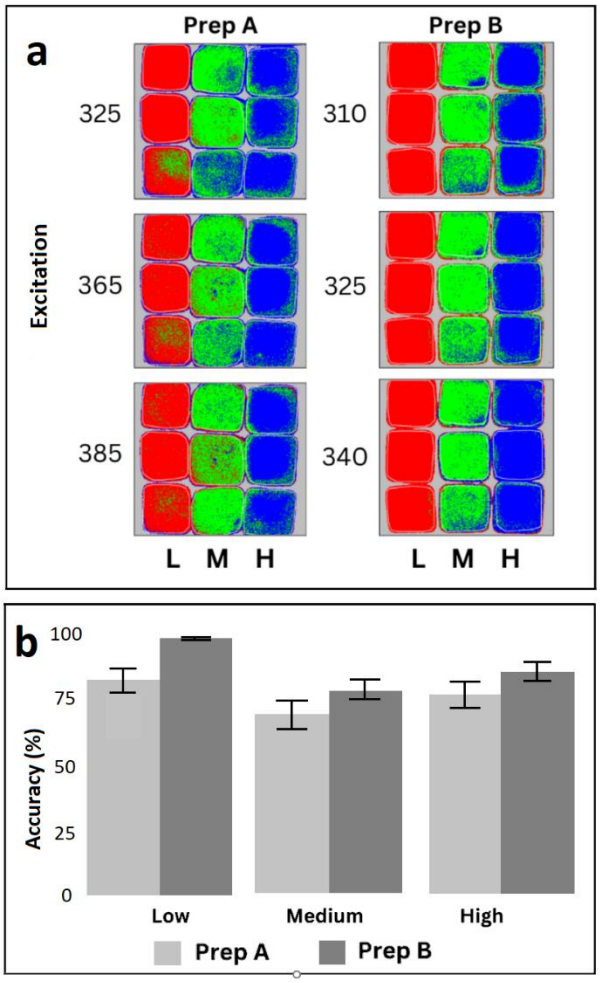


Fig. 5. (a) SVM classification maps obtained with the three best single excitations for each preparation, using 31 emission bands. Red, green and blue: pixels assigned to low (L), medium (M) and high (H) crosslinking. (b) Per-class accuracy (mean ± SD) for Prep A and Prep B.

3.3. Classification with combined excitations

Combining excitations improved classification (**Fig. 6**). For Prep A, the best performance was obtained by incorporating all six excitations, with accuracies of 92%, 92% and 95% for the low, medium and high crosslinker levels. For Prep B, ME-HSI also improved discriminative capacity, particularly

when only the three best excitations (310, 325 and 340 nm) were used.

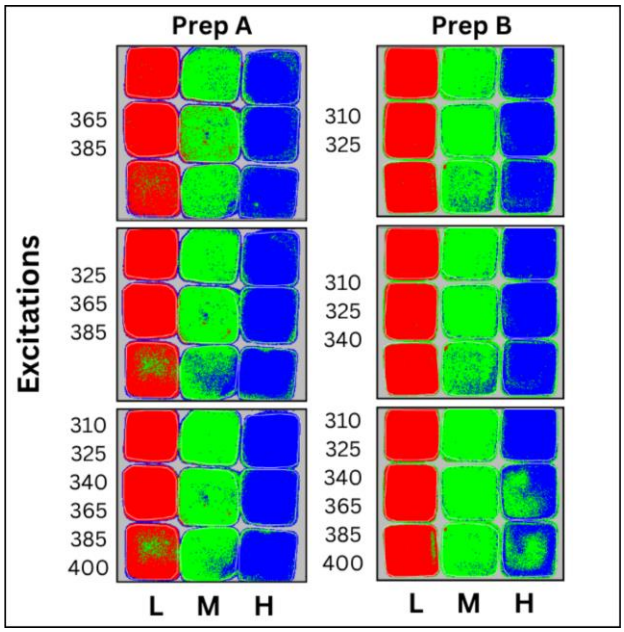


Fig. 6. SVM classification maps obtained with combinations of the best-performing excitations and all their emission bands.

When all six excitations were combined, the model remained accurate for both groups, but specifically for scaffolds prepared without pepsin (**Fig.7**). Accuracy increased from about 53% with two features to about 86% with 31, and a combination of only 10 features yielded 75% accuracy, which was sufficient to visually discriminate the scaffolds.

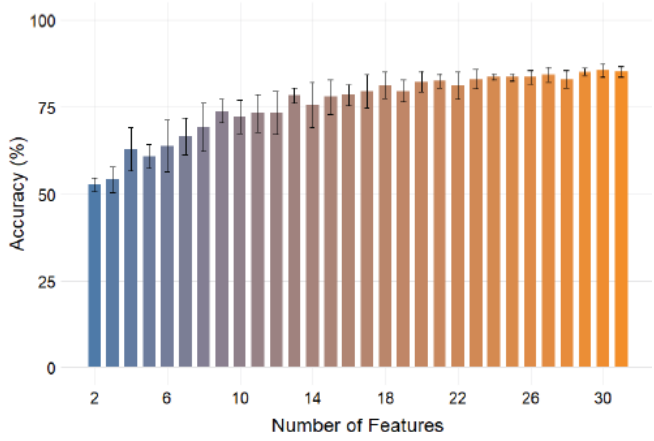


Fig. 7. Classification accuracy (mean ± SD) as a function of the number of emission features, using all six excitations.

4. DISCUSSION

Glutaraldehyde crosslinking produced only subtle changes in the mean autofluorescence spectra of collagen sponges, but these changes were sufficient for pixel-level classification of three crosslinker levels. Two observations stand out. First, the discriminative power depended strongly on excitation wavelength: the classes were most visibly different at 365 and 385 nm, whereas 400 nm excitation separated pixels from samples treated with low GA concentrations, but could not resolve pixels from samples treated with medium and high GA concentrations. Second, the most discriminative excitations depended on how the collagen was extracted. Pepsin-aided extraction removes the telopeptide regions of the collagen molecule, where native intermolecular crosslinks form, so the two preparations likely start from different fluorophore contents. This may explain why Prep B was best classified at 310–340 nm and Prep A at 325–385 nm excitation ranges.

Combining excitations improved accuracy over the best single excitation, consistent with our earlier ME-HSI results on nerve, ligament and lichen specimens [8]–[10]. The accuracy obtained with only 10 emission bands across six excitations suggests that a small set of excitation–emission pairs may suffice for routine scaffold assessment, which is relevant for designing simpler, dedicated instruments.

The present excitation range might not capture the entire crosslinking-induced shifts in collagen fluorescence. Yet even excitation–emission combinations outside the deep-UV range were sufficient to distinguish the degrees of crosslinking tested here. Scaffolds with higher degrees of crosslinking might require additional or longer-wavelength excitation sources for best discrimination.

Looking at **Fig.1** one might notice small visual differences in surface texture observed between the sponges. These are likely to arise from the physical dynamics of the lyophilization (freeze-drying) process. Specifically, intermediate glutaraldehyde concentrations induce a moderate degree of polymer network stabilization that alters initial ice crystal nucleation rates and sublimation kinetics compared to the loosely crosslinked or highly densely crosslinked scaffolds. Meniscus variations during manual casting in multiwell molds can also result in localized thickness variations. Therefore, we have conducted additional sets of experiment to confirm that classification models used here also work on collagen scaffolds prepared on separate days, subjected to independent lyophilization cycles, or imaged during different acquisition sessions under identical optical parameters [13]. The classification model maintained high robustness and accuracy on these difference batches, confirming that the identified spectral features reflect true biochemical differences rather than session-specific artifacts or overfitting. Importantly, because hyperspectral imaging approach evaluates pixel-level spatial spectra and uses normalization per cube, these localized physical and textural variations do not compromise the biochemical classification accuracy. In contrary they highlight the importance of automated, non-destructive

quality control methods capable of revealing degree of crosslinking despite structural heterogeneities.

Lastly, the array setup used in this study maintained a fixed geometric layout of sponges. To address possible positional bias we also tested the impact of rotating samples across different spatial positions within the field of view (including center and peripheral locations). The results confirmed that classification performance remains stable and independent of precise physical placement within the imaging area, verifying that the model relies on intrinsic biochemical autofluorescence shifts rather than spatial illumination gradients.

5. CONCLUSION

Hyperspectral imaging under multiple excitation wavelengths captured distinct spectral profiles of collagen scaffolds prepared with different crosslinker concentrations. The data point to autofluorescence-based ME-HSI as a tool for non-destructive, spatially resolved quality control of collagen-based biomaterials. Computational analysis showed that discrimination was highly dependent on excitation wavelength, and that the most discriminative excitations differ between collagen preparation methods.

6. ACKNOWLEDGMENT

The authors gratefully acknowledge support from the ERA Chair project NAR-SAR-IPH, funded by the European Union (Project No. 101087403), and the Research Support Grant for PhD Candidates (Project No. 25AA-1F080), awarded by the Higher Education and Science Committee of the MESCS RA.

7. REFERENCES

[1] J. Glowacki and S. Mizuno, "Collagen scaffolds for tissue engineering," *Biopolymers*, vol. 89, no. 5, pp. 338–344, 2008.

[2] L. H. H. Olde Damink *et al*., "Glutaraldehyde as a crosslinking agent for collagen-based biomaterials," *J. Mater. Sci.: Mater. Med.*, vol. 6, pp. 460–472, 1995.

[3] H. Ju, X. Liu, G. Zhang, D. Liu, and Y. Yang, "Comparison of the structural characteristics of native collagen fibrils derived from bovine tendons using two different methods: modified acid-solubilized and pepsin-aided extraction," *Materials*, vol. 13, no. 2, p. 358, 2020.

[4] Ł. Saletnik, W. Szczęsny, J. Szmytkowski, and J. J. Fisz, "On the nature of stationary and time-resolved fluorescence spectroscopy of collagen powder from bovine Achilles tendon," *Int. J. Mol. Sci.*, vol. 24, no. 8, p. 7631, 2023.

[5] Y. Shen, D. Zhu, W. Lu, B. Liu, Y. Li, and S. Cao, "The characteristics of intrinsic fluorescence of type I collagen influenced by collagenase I," *Appl. Sci.*, vol. 8, no. 10, p. 1947, 2018.

[6] G. Saiko, P. Lombardi, Y. Au, D. Queen, D. Armstrong, and K. Harding, "Hyperspectral imaging in wound care: a systematic review," *Int. Wound J.*, vol. 17, no. 6, pp. 1840–1856, 2020.

[7] M. Jayachandran, S. Rodriguez, E. Solis, J. Lei, and A. Godavarty, "Critical review of noninvasive optical technologies for wound imaging," *Adv. Wound Care*, vol. 5, no. 8, pp. 349–359, 2016.

[8] N. Chilingaryan, F. Villarruel, T. Soghomonyan, V. Yeghiazaryan, and N. Sarvazyan, "4D hyperspectral imaging for intraoperative tissue classification," in *Proc. SPIE*, vol. 13410, p. 134100Z, 2025.

[9] N. Matosyan, N. Chilingaryan, N. Sarvazyan, and V. Yeghiazaryan, "Combining 4D hyperspectral imaging with CNN for nerve and ligament differentiation," in *Proc. IEEE ISBI*, 2025.

[10] N. Chilingaryan, A. Gasparyan, and N. Sarvazyan, "Multi-excitation hyperspectral imaging toward improved lichen identification," in *Proc. IEEE WHISPERS*, 2025, pp. 1–5.

[11] L. van der Maaten and G. Hinton, "Visualizing data using t-SNE," *J. Mach. Learn. Res.*, vol. 9, pp. 2579–2605, 2008.

[12] C. Cortes and V. Vapnik, "Support-vector networks," *Mach. Learn.*, vol. 20, no. 3, pp. 273–297, 1995.

[13] Kristina Ghahramanyan. (2026). 260319_ME-HSI acquisition of crosslinked collagen biomaterials [Dataset]. *Zenodo*. https://doi.org/10.5281/zenodo.22108150